Electrochemical incineration of cresols: A comparative study between PbO2 and boron-doped diamond anodes

Cristina Flox, Conchita Arias, Enric Billas, André Savall, Karine Groenen Serrano

Electrochemical incineration of cresols: A comparative study between PbO_2 and boron-doped diamond anodes

Cristina Flox [a], Conchita Arias [a], Enric Brillas [a], André Savall [b], Karine Groenen-Serrano [b,*]

[a] *Laboratori d'Electroquímica dels Materials i del Medi Ambient, Departament de Química Física, Facultat de Química, Universitat de Barcelona, Martí i Franquès 1-11, 08028 Barcelona, Spain*
[b] *Laboratoire de Génie Chimique, CNRS, Université Paul Sabatier 118, Route de Narbonne, 31062 Toulouse Cedex 9, France*

A B S T R A C T

The electrooxidation of aqueous solutions containing 5 mM of *o*-, *m*- and *p*-cresol at pH 4.0 has been investigated using a flow filter-press reactor with a boron-doped diamond (BDD) under galvanostatic electrolysis. All cresols are degraded at similar rate up to attaining overall mineralization. Comparable treatment of the *m*-cresol effluent on PbO_2 leads to partial electrochemical incineration. However, this pollutant is more rapidly removed with PbO_2 than with BDD. The decay kinetics of all cresols follows a pseudo-first-order reaction. Aromatic intermediates such as 2-methylhydroquinone and 2-methyl-*p*-benzoquinone and carboxylic acids such as maleic, fumaric, pyruvic, malonic, tartronic, glycolic, glyoxylic, acetic, oxalic and formic, have been identified and followed during the *m*-cresol treatment by chromatographic techniques. From these oxidation by-products, a plausible reaction sequence for *m*-cresol mineralization on both anodes is proposed. The energy consumption for the corresponding electrochemical process is also calculated.

1. Introduction

Phenol and its derivatives are the major constituents of industrial wastewater produced by oil refineries, petrochemicals, polymeric resins, pharmaceuticals, coal conversion plants and chemical industries (Rajkumar and Palanivelu, 2003; Ródenas-Torralva et al., 2005; Wu et al., 2006). Their high aqueous solubility and weak adsorption to most soils result in a quick entry into groundwater due to leaching (Rao and Asolekar, 2001). The concentration of these compounds in agro-industrial wastewaters can vary from 0.05 to 10 g L^{-1} depending on the type and origin of the effluent. In a contaminated aquifer of Fredensborg (Denmark), for example, phenol, *o*-cresol and *m*-cresol contents of 2.00, 0.65 and 0.78 mg L^{-1}, respectively, were detected (Flyvbjerg et al., 1993). For a low temperature coal carbonization wastewater, about 2.5 g L^{-1} phenol, 250 mg L^{-1} resorcinol, 5.3 g L^{-1} catechol, 480 mg L^{-1} *o*-cresol, 200 mg L^{-1} *m*-cresol, 470 mg L^{-1} *p*-cresol, 2.0 g L^{-1} pyrogallol and 400 mg L^{-1} xylenol were found (Rajkumar et al., 2005). High phenol, *p*-cresol and resorcinol concentrations were also determined in wastewaters coming from the oil shale treatment process.

At concentrations above some threshold levels, phenolic compounds are toxic to microorganisms and refractory to biodegradation. Cresols are classified by the US EPA as persistent, priority and toxic chemicals, showing chronic effects at 12 mg L^{-1} of the quantitative structure–activity relationship (Kavitha and Palanivelu, 2005). Unfortunately, the high contamination of industrial wastewaters of these compounds, their seasonal production and the presence of other organic pollutants such as lipids usually render these effluents inappropriate for direct biological treatment. Alternative powerful oxidation technologies are then needed to be developed for achieving total destruction of cresols from wastewaters.

Advanced oxidation processes (AOPs) based on the in situ generation of hydroxyl radical (·OH) are promising environmentally friendly techniques for water remediation. ·OH is the second strongest oxidant known after fluorine, with a high standard potential ($E°$ = 2.80 V vs. SHE) that makes feasible its fast non-selective reaction with organics to give dehydrogenated or hydroxylated by-products up to total mineralization, i.e., conversion into CO_2 and water.

Several papers have reported the rapid removal of *o*-, *m*- and/or *p*-cresol from waters by photocatalysis with TiO_2/UV. Hatipoğlu et al. (2004) found that *m*-cresol undergoes a 74% decay after 160 min of treatment by this AOP following a pseudo-first-order kinetics and proposed the initial generation of 3-methylcathecol from quantum mechanical calculations. In contrast, mixtures of hydroxylated and benzoquinone derivatives have been detected by gas chromatography–mass spectrometry (GC–MS) from the photocatalytic degradation of all cresols (Wang et al., 1998; Sivalingam et al., 2004). The treatment of wastewaters of these

* Corresponding author. Tel.: +33 561558677; fax: +33 561556139.
E-mail address: serrano@chimie.ups-tlse.fr (K. Groenen-Serrano).

compounds by other AOP such as Fenton's reagent (H_2O_2/Fe^{2+}) only allows attaining 42% mineralization, because of the production of acetic and oxalic acids as major by-products, which are difficulty destroyed by ·OH formed in the bulk (Kavitha and Palanivelu, 2005). In this scenario, we previously reported that total mineralization of cresols is feasible using the solar photoelectro-Fenton method in which complexes of Fe(III) with generated carboxylic acids are efficiently photodecomposed by UV irradiation of sunlight (Flox et al., 2007).

Electrochemical oxidation or electrooxidation is the most popular electrochemical treatment for wastewaters containing low contents of organics. This AOP allows the electrochemical incineration of pollutants from their mediated oxidation with hydroxyl radical formed at a high O_2-overvoltage anode (M) from water oxidation (Panizza and Cerisola, 2005):

$$M(H_2O) \rightarrow M(^{\cdot}OH) + H^+ + e^- \quad (1)$$

Recently, electrooxidation has received great attention due to the use of non-active boron-doped diamond (BDD) thin film electrodes, which possess so high O_2-overvoltage that favors the production of great quantity of reactive BDD(·OH) with ability to completely mineralize organics, as shown for several aromatics (Panizza et al., 2001; Marselli et al., 2003; Polcaro et al., 2003; Brillas et al., 2005; Flox et al., 2006; Nava et al., 2007; Zhao et al., in press) and carboxylic acids (Martinez-Huitle et al., 2004; Weiss et al., 2007). Thus, Nava et al. (2007) described the efficient electrochemical incineration of 2 mM *p*-cresol and *o*-cresol in 1 M H_2SO_4 using a filter-press-type FM01-LC cell with a BDD anode and a Ti/Pt cathode, both of 64 cm^2 area. After 3 h of electrolysis at 10 mA cm^{-2}, *p*-cresol reached 90% mineralization, with 71% current efficiency and an energy consumption of 7.84 kW h m^{-3}; whereas *o*-cresol was mineralized to 84%, with 67% current efficiency and 6.56 kW h m^{-3} energy cost. However, no intermediates were detected in these trials. These results evidence the good performance of a BDD anode for treating cresols wastewaters. In contrast, a poor electrochemical degradation for *o*-, *m*- and *p*-cresol in alkaline medium with generation of hypochlorite ion as oxidant has been found by Rajkumar and Palanivelu (2003) using an undivided cell with a Ti/TiO_2–RuO_2–IrO_2 anode and a graphite cathode. At pH 9 the optimum operating conditions yielding maximum degradation, shorter electrolysis time and less energy consumption were achieved with 2.5 g L^{-1} chloride as electrolyte and cresols concentration >300 mg L^{-1} at 54 mA cm^{-2} (1.5 A). The chemical oxygen demand decreased in the sequence: *m*-cresol > *o*-cresol > *p*-cresol, but total organic carbon (TOC) removal values as low as 50–60% were obtained after the consumption of high specific charges of 40–50 Ah L^{-1}. Adsorbable organic halogens analysis of treated solutions revealed the production of chloroderivatives as intermediates.

The good performance of other potent anodes such as PbO_2 in electrooxidation for the removal of phenol and other organics has been confirmed previously and compared with the oxidation power of BDD anodes (Belhadj Tahar and Savall, 1998; Belhadj Tahar et al., 2008; Martinez-Huitle et al., 2008; Sirés et al., 2008; Weiss et al., 2008; Zhu et al., 2008). To gain a better knowledge on the ability of these anodes to oxidize phenolic compounds, we have undertaken the present study on the electrochemical incineration of cresols in acid medium using a flow filter-press reactor under galvanostatic conditions. Our research was focused to determine the degradation rate of *o*-, *m*- and *p*-cresol effluents with BDD to be further compared with that of *m*-cresol with PbO_2. A concentrated (5 mM) solution of each pollutant was treated to clarify the role of aromatic intermediates and carboxylic acids formed on the degradation process. The decay kinetics of all cresols and the evolution of by-products for *m*-cresol were then followed by chromatographic techniques, allowing the proposal of a reaction pathway for *m*-cresol mineralization. The energy consumption for the electrochemical treatment of this compound on each anode was also calculated.

2. Experimental

2.1. Chemicals

o-Cresol (99% purity), *m*-cresol (99% purity) and *p*-cresol (97% purity) were purchased from Sigma and used in the electrochemical trials as received. 2-Methylhydroquinone, 2-methyl-*p*-benzoquinone and maleic, fumaric, malic, malonic, tartronic, pyruvic, glycolic, glyoxylic, acetic and oxalic acids were either reagent or analytical grade from Sigma–Aldrich, Merck and Avocado. Solutions were prepared with high-purity water obtained from a Millipore Milli-Q system (resistivity > 18 MΩ cm at 25 °C). Analytical grade sulfuric acid from Prolabo was used to adjust its initial pH to 4.0. Anhydrous sodium sulfate employed as background electrolyte was analytical grade supplied by Prolabo. Other chemicals and organic solvents were either HPLC or analytical grade from Sigma–Aldrich, Merck and Prolabo.

2.2. Electrochemical reactor

Electrolyses were conducted in a one-compartment flow filter-press reactor (Diacell) under galvanostatic conditions and in batch operation mode. Electrodes were two discs of 63 cm^2 of active surface separated 10 mm. The anode was either a Si wafer coated with a 1 μm BDD thin layer or a titanium disc covered with a PbO_2 film supplied by De Nora. The BDD electrode from Centre Suisse d'Électronique et de Microtechnique (Neuchâtel, Switzerland) was elaborated by chemical vapour deposition on a conductive substrate of polysilicium. The cathode was a 1 mm thick disc of zirconium. The current was supplied by an ELC AL 924 power supply. Details on the electrochemical system are reported elsewhere (Weiss et al., 2007).

Comparative degradation of cresols was studied by electrolyzing 1 L of solutions containing 5 mM of initial pollutant and 0.05 M Na_2SO_4 of pH 4.0. In all trials, a constant current density of 40 mA cm^{-2} was applied. The solution temperature was maintained at 25 °C and the effluent was recirculated at a constant flow rate of 126 L h^{-1}.

2.3. Analysis procedures

The solution pH was determined with a Schott pH-meter CG 837. Samples withdrawn from original and treated solutions were filtered with Whatman 0.45 μm PTFE filters before analysis. The mineralization of cresols solutions was monitored from the decay of their dissolved organic carbon (DOC), determined on a Shimadzu 5050A TOC analyzer with 2% accuracy.

The organic components of about 100 mL of the 5 mM *m*-cresol solution treated with a BDD anode for 60 min were extracted three times with 25 mL of CH_2Cl_2. The collected organic solution was dried with anhydrous Na_2SO_4, filtered and rotavaporated up to ca 2 mL. The remaining aromatic intermediates were further identified by GC–MS using a Hewlett-Packard 5890 Series II gas chromatograph fitted with an Elite-5MS 0.25 μm, 30 m × 0.25 mm (i.d.), column, and a Hewlett-Packard 5989A mass spectrophotometer operating in electron impact mode at 70 eV. The temperature ramp for this column was 70 °C for 1 min, 20 °C min^{-1} up to 250 °C and hold time 1 min. The evolution of all cresols and aromatic intermediates from *m*-cresol were followed by reversed-phase HPLC chromatography using a Hewlett-Packard 1100 Series liquid chromatograph, fitted with a Spherisorb ODS2 5 μm, 150 mm ×

4.6 mm (i.d.), column at room temperature, equipped with an UV/Vis detector selected at λ = 276 nm and controlled with an Agilent ChemStation software. These measurements were made by injecting 20 μL aliquots and circulating a 50:45:5 (v/v/v) methanol/phosphate buffer (pH 2.5)/pentanol mixture at 1.0 mL min^{-1} as mobile phase. Carboxylic acids were detected by ion-exclusion chromatography using the same HPLC system fitted with a Supelcogel C-610H 9 μm, 300 mm × 7.8 mm (i.d.), column at 35 °C, selecting the UV/Vis detector at 210 nm and under circulation of 0.018 M H_3PO_4 at 0.5 mL min^{-1} as mobile phase.

3. Results and discussion

3.1. Comparative degradation of cresols

A series of comparative electrolyses for all cresols was performed using the BDD anode to test if the relative position of –CH_3 and –OH groups has any effect on the oxidation rate of these compounds. Solutions containing 415 mg L^{-1} DOC of each cresol of pH 4.0 were treated at 40 mA cm^{-2}, 25 °C and liquid flow rate of 126 L h^{-1} by prolonging the electrolysis time to attain almost overall decontamination. In these trials the solution pH remained practically constant and the starting colorless solutions changed to a clear brown color after 1 h of electrolysis, becoming colorless again at the end of treatment. This change in solution color can be related to the formation of benzoquinone intermediates, as will be discussed below.

The DOC abatement as function of the consumed specific charge obtained for the above experiments is depicted in Fig. 1. A fast and quite similar DOC decay can be observed for all solutions, yielding more than 98% mineralization after consumption of 22 Ah L^{-1} for 8 h. These findings evidence that all cresols undergo an analogous degradation process on BDD since BDD(·OH) formed from water oxidation by reaction (1) is able to completely mineralize these compounds at similar rate.

In order to compare the oxidation ability of BDD and PbO_2, a commercially and more available material, we decided to investigate the degradation of *m*-cresol using the latter anode. In this case, the effluent acquired an intense dark brown color and a black precipitate, probably composed of polymeric by-products, was slowly formed during the first hour of electrolysis. As illustrated in Fig. 1, the use of PbO_2 leads to a slow DOC decay, only attaining 68% decontamination of the *m*-cresol effluent at 27 Ah L^{-1} (10 h). This behaviour clearly differs from that found for BDD, which has much higher oxidation power to destroy all organics present in the medium along the electrolysis. Since a similar performance is expected for the other two cresol isomers using PbO_2, without achieving overall mineralization, only the oxidation process of *m*-cresol and its intermediates was comparatively studied for both anodes, as reported below.

3.2. Decay kinetics of cresols

The kinetics of the reaction of initial pollutants with BDD(·OH) or PbO_2(·OH) under the above operating conditions was followed by reversed-phase HPLC, where *o*-, *m*- and *p*-cresol exhibited a well-defined absorption peak at retention time (t_r) of 3.7, 3.5 and 3.6 min, respectively. The change of concentration of these compounds with electrolysis time is given in Fig. 2. As can be seen, all cresols are removed at similar rate with BDD, disappearing from the medium at the same time close to 480 min. It is worth noting that the time required for total removal of *o*-, *m*- and *p*-cresol with BDD is very similar to that needed for their overall mineralization, indicating that cresols persist in solution up to the end of the combustion process and they are degraded in parallel to their by-products by BDD(·OH). However, Fig. 2 shows that *m*-cresol appears to be destroyed at slightly greater rate using a PbO_2 anode and completely removed in a shorter time of 420 min, despite its much slower DOC removal (see Fig. 1). It is well known that ·OH formed at BDD remains mainly free on its surface where it attacks non-selectively and directly organics, whereas this radical is adsorbed on the PbO_2 surface, where it reacts selectively and more slowly with adsorbed organics (Flezar and Plosyznska, 1985; Zhu et al., 2008). According to this behaviour, several authors (Zhu et al., 2008; Martinez-Huitle et al., 2008) recently reported that phenol, *p*-substituted phenols and pesticide methamidophos are more rapidly destroyed with BDD than with PbO_2 using small conventional electrolytic cells. In contrast, results of Fig. 2 indicate a quite similar destruction rate for *m*-cresol using both anodes, as also found by us for phenol decay operating with the same flow cell under analogous conditions (Weiss et al., 2008). The enhancement of *m*-cresol removal using PbO_2 in our system can then be explained in the same way as previously justified for phenol, that is, by the increase in the mass transfer coefficient of substrate owing to the higher O_2 evolution produced on PbO_2 than on BDD.

The above concentration decays were well-fitted to a pseudo-first-order kinetic equation and the excellent straight lines thus ob-

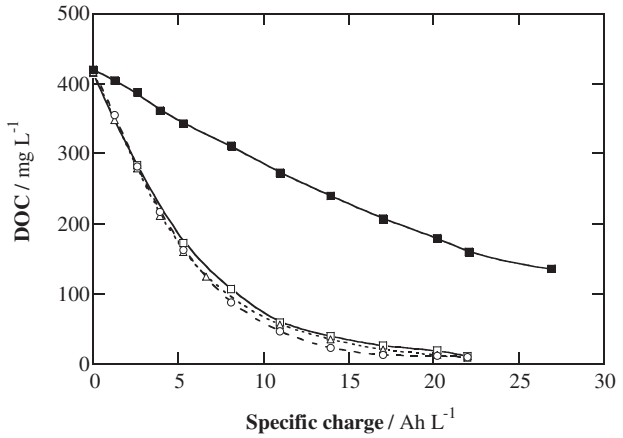

Fig. 1. Dissolved organic carbon removal for the electrochemical incineration of 1 L of solutions with 5 mM of (○) *o*-cresol, (□, ■) *m*-cresol and (△) *p*-cresol in 0.05 M Na_2SO_4 of pH 4.0. The flow reactor was a filter-press cell with a (○, □, △) BDD or (■) PbO_2 anode and a Zr cathode (all them of 63 cm^2 area) operating at 40 mA cm^{-2} and 25 °C in batch mode at liquid flow rate of 126 L h^{-1}.

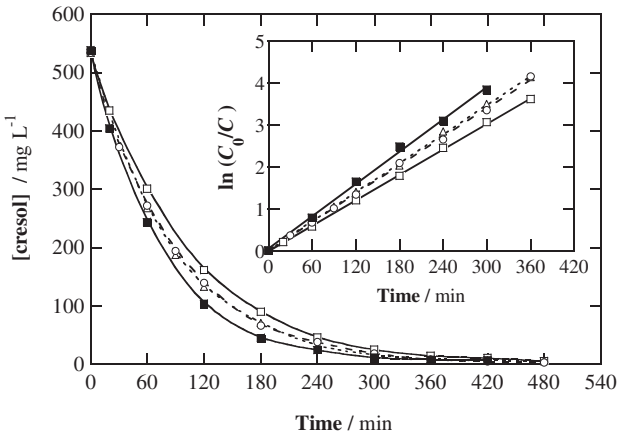

Fig. 2. Decay of *o*-, *m*- and *p*-cresol concentrations with electrolysis time for the trials reported in Fig. 1. The inset panel shows the kinetic analysis for the corresponding experiments assuming a pseudo-first-order reaction for each initial compound.

tained are depicted in the inset panel of Fig. 2. This suggests the production of a constant ·OH concentration at each anode during electrolysis, which is much higher than that of the initial pollutant reacting with it either on the PbO_2 surface or in the vicinity of the BDD electrode (Weiss et al., 2008). From this analysis, a similar pseudo-first-order rate constant (k_1) of $1.89 \times 10^{-4}\ s^{-1}$ (square regression coefficient $R^2 = 0.9993$) for *o*-cresol, $1.69 \times 10^{-4}\ s^{-1}$ ($R^2 = 0.9996$) for *m*-cresol and $1.93 \times 10^{-4}\ s^{-1}$ ($R^2 = 0.9990$) for *p*-cresol was determined for BDD, whereas a slightly higher $k_1 = 2.14 \times 10^{-4}\ s^{-1}$ ($R^2 = 0.9978$) for *m*-cresol was found for PbO_2. The quite analogous k_1-values obtained for all cresols using a BDD anode evidence that they undergo the same kind of attack by BDD(·OH), then leading to the production of similar primary aromatic by-products. In literature, quite similar second-order constant rate (k_2) values of 1.1×10^{10} and $1.2 \times 10^{10}\ M^{-1}\ s^{-1}$ have also been determined for the homogeneous reaction of hydroxyl radical with *o*-cresol (Savel'eva et al., 1972) and *p*-cresol (Feitelson and Hayon, 1973), respectively.

The above kinetic behaviour has also been described by Polcaro et al. (2003) for the removal of phenol solutions with BDD under galvanostatic electrolysis, reporting a k_1-value of $1.94 \times 10^{-4}\ s^{-1}$. In our previous studies on the comparative performance of the same electrode materials on phenol degradation (Weiss et al., 2008), it was found that this pollutant disappears at similar rate using both anodes, although in terms of DOC removal, BDD becomes more effective. All these results suggest that phenol and cresols are attacked by BDD(·OH) and PbO_2(·OH) in the same way, although the by-products formed are more easily destroyed by the former.

On the other hand, it is well known (Panizza et al., 2001; Panizza and Cerisola, 2005; Flox et al., 2006; Weiss et al., 2008) that electrogenerated ·OH dimerizes to H_2O_2 by reaction (2). This species can then be oxidized to O_2 via reaction (3) or can react with ·OH to give hydroperoxyl radical ($HO_2^{\cdot}$) from reaction (4). Apart from the weak oxidants H_2O_2 and $HO_2^{\cdot}$ thus produced, the high oxidation power of BDD favors the generation of other weaker oxidizing species than ·OH, like peroxodisulfate ion ($S_2O_8^{2-}$) from the oxidation of SO_4^{2-} and HSO_4^- ions from the electrolyte by reactions (5) and (6), respectively (Serrano et al., 2002), and ozone by reaction (7).

$$2{\cdot}OH \rightarrow H_2O_2 \quad (2)$$

$$H_2O_2 \rightarrow O_2 + 2\,H^+ + 2\,e^- \quad (3)$$

$$H_2O_2 + {\cdot}OH \rightarrow HO_2^{\cdot} + H_2O \quad (4)$$

$$2SO_4^{2-} \rightarrow S_2O_8^{2-} + 2e^- \quad (5)$$

$$2HSO_4^- \rightarrow S_2O_8^{2-} + 2H^+ + 2e^- \quad (6)$$

$$3H_2O \rightarrow O_{3(g)} + 6H^+ + 6e^- \quad (7)$$

We have confirmed that cresols do not react directly with H_2O_2 and $S_2O_8^{2-}$, because no change of their concentrations in separated solutions containing 20 mM of each oxidant has been observed by reversed-phase HPLC. Since ozone is a very weak oxidant in acid medium, one can infer that electrogenerated BDD(•OH) and PbO_2(·OH) from reaction (1) are the main species producing the degradation of cresols under our experimental conditions. The fact that the solutions of these compounds can be completely mineralized with BDD, but only partially decontaminated with PbO_2, evidence that waste reactions (2)–(4) are less important for BDD(·OH) than for PbO_2(·OH) (Weiss et al., 2008).

3.3. Identification and evolution of intermediates for m-cresol degradation

To clarify the different ability of BDD and PbO_2 anodes to mineralize cresols, we concentrated our efforts to identify and follow the aromatic intermediates and carboxylic acids produced during *m*-cresol degradation.

GC–MS analysis of the *m*-cresol solution treated for 1 h with BDD revealed the formation of two aromatic intermediates, 2-methylhydroquinone ($m/z = 124$ (100, M^+)) at $t_r = 6.8$ min and its oxidation product 2-methyl-*p*-benzoquinone ($m/z = 122$ (100, M^+)) at $t_r = 4.7$ min. These stable by-products were confirmed in the reversed-phase HPLC chromatograms of the treated solutions, which displayed two well-defined peaks related to 2-methylhydroquinone at $t_r = 1.8$ min and 2-methyl-*p*-benzoquinone at $t_r = 2.4$ min, identified from comparison of their t_r-values with those of pure compounds. Note that these compounds have also been reported for the oxidation of *m*-cresol with ·OH produced from TiO_2/UV (Wang et al., 1998; Sivalingam et al., 2004) and H_2O_2/Fe^{2+} (Flox et al., 2007).

Fig. 3 illustrates the change in concentration of 2-methylhydroquinone and 2-methyl-*p*-benzoquinone during the degradation of the *m*-cresol solutions. Both compounds are accumulated to about 0.7 and 1.1 mg L^{-1} as maximum, respectively, at 60 min of treatment with BDD, further being slowly removed to disappear in 360–420 min, that is, a time similar to that needed for the total removal of the initial pollutant (see Fig. 2). The same trend can be observed for these by-products in Fig. 3 when PbO_2 is used, although in this case maximum contents of ca 2.5 and 92 mg L^{-1} are accumulated, respectively, indicating that 2-methyl-*p*-benzoquinone is more hardly oxidized with PbO_2(·OH) than with BDD(·OH).

Ion-exclusion HPLC chromatograms of the same treated solutions exhibited peaks corresponding to oxalic ($t_r = 9.3$ min), tartronic ($t_r = 11.4$ min), maleic ($t_r = 12.1$ min), pyruvic ($t_r = 13.3$ min), glyoxylic ($t_r = 13.8$ min), malonic ($t_r = 14.8$ min), glycolic ($t_r = 17.8$ min), formic ($t_r = 19.8$ min), acetic ($t_r = 21.1$ min) and fumaric ($t_r = 23.3$ min) acids. While pyruvic, malonic, maleic, fumaric and glycolic acids are formed from the degradation of the aryl moiety of aromatic intermediates (Brillas et al., 2005; Flox et al., 2006), acetic, tartronic and glyoxylic acids come from the oxidation of pyruvic, malonic and glycolic acids, respectively (Boye et al., 2002; Flox et al., 2006). These acids are independently converted into oxalic and formic acids, which are directly mineralized to CO_2 as ultimate carboxylic acids.

The time-course of the concentration of relevant carboxylic acids determined using BDD and PbO_2 is presented in Fig. 4a and b, respectively. As can be seen, most acids are more rapidly removed with BDD(·OH) than with PbO_2(·OH). For example, pyruvic acid was only found along 480 min of electrolysis with PbO_2 (see

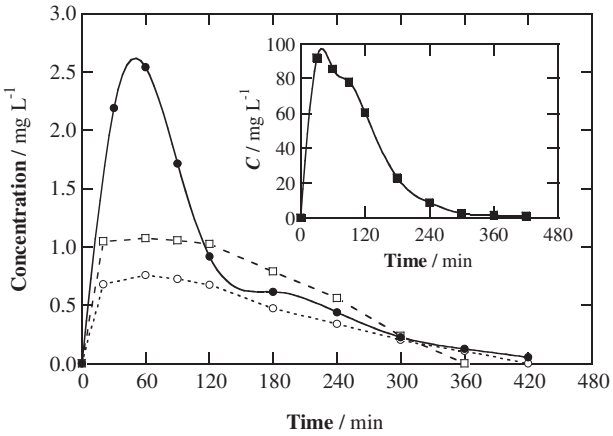

Fig. 3. Evolution of the concentration of aromatic intermediates detected during the degradation of 1 L of 534 mg L^{-1} of *m*-cresol in 0.05 M Na_2SO_4 at pH 4.0 in a flow cell at 40 mA cm^{-2}, 25 °C and liquid flow rate of 126 L h^{-1}. Compound: (○, ●) 2-methylhydroquinone; (□, ■) 2-methyl-*p*-benzoquinone. Anode: BDD (empty symbols); PbO_2 (full symbols).

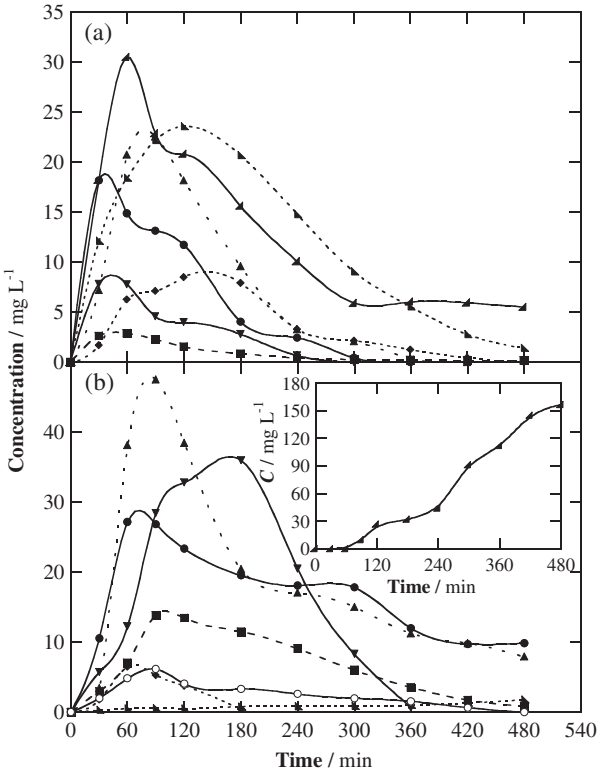

Fig. 4. Time-course of the concentration of relevant carboxylic acids detected during the electrochemical incineration of 1 L of a 534 mg L^{-1} *m*-cresol solution under the same conditions of Fig. 3 using a (a) BDD or (b) PbO_2 anode. Acid: (♦) tartronic; (■) maleic; (●) malonic; (○) pyruvic; (▼) glycolic; (▲) glyoxylic; (◢) acetic; and (◣) oxalic.

Fig. 4b), but it was undetected using a BDD anode. The same trend was found for fumaric acid (not shown in Fig. 4), which attained a maximum content of 0.6 mg L^{-1} at 180 min in the former case. Formic acid was so rapidly destroyed on both anodes that it was only detected at trace level during the first 60 min of electrolysis. A very different behaviour can be seen in Fig. 4a and b for acetic and oxalic acids. In the case of BDD the concentration of the first acid rises rapidly to ca 30 mg L^{-1} at 60 min and further slowly falls to near 5 mg L^{-1} at 480 min, whereas oxalic acid is almost completely removed at this time after attaining a maximum content of approximately 23 mg L^{-1} at 120 min. That means that the final electrolyzed solution with BDD is mainly composed of acetic acid with less than 2% of the initial DOC (see Fig. 1). When a PbO_2 anode is used, however, acetic acid is continuously accumulated up to ca 155 mg L^{-1} at 480 min, as expected if this acid is not destroyed by PbO_2(·OH). Under these conditions, Fig. 4b also shows the presence of a very low oxalic acid concentration (<2 mg L^{-1}), which can be ascribed to its fast anodic oxidation owing to its strong interaction with the PbO_2 surface (Martinez-Huitle et al., 2004). Although oxalic acid possesses a very weak reactivity with homogeneous hydroxyl radicals (Getoff et al., 1971), our results evidence that it can then be converted into CO_2 by BDD(·OH) and even much more quickly by PbO_2(·OH), where probably it is adsorbed. In the same manner, Zhao et al. (in press) showed that the electrochemical incineration of phenol leads to the formation of less variety of intermediates using BDD than a Pt anode, which destroys much more slowly all by-products owing to its much lower oxidation ability. The use of ultrasound coupled with electrolysis enhanced the degradation rate of phenol on BDD by 301%, but without changing the amount of intermediates species formed.

Fig. 5a and b present a comparison between the experimental DOC values for *m*-cresol degradation and the calculated ones from the remaining concentration of this compound and of its oxidation by-products determined by HPLC for BDD and PbO_2, respectively. Both measured and calculated data are in good agreement for BDD, being the △DOC difference always lower than 16 mg L^{-1}, as illustrated in Fig. 5c. Since the main contribution to DOC comes from the remaining initial pollutant in the effluent (see Fig. 5a), one can infer that the electrochemical combustion of *m*-cresol takes place practically at the same rate as it is oxidized by BDD(·OH). This radical is then able to destroy rapidly all intermediates, as shown in Figs. 3 and 4a for the main by-products detected. In the case of PbO_2, Fig. 5b shows that the experimental DOC cannot be accounted for by the faster loss of *m*-cresol and the higher content of accumulated carboxylic acids. A △DOC difference as high as 170 mg L^{-1} is found at 180 min of electrolysis. These findings evidence that a large amount of other undetected intermediates are produced under these conditions due to the low

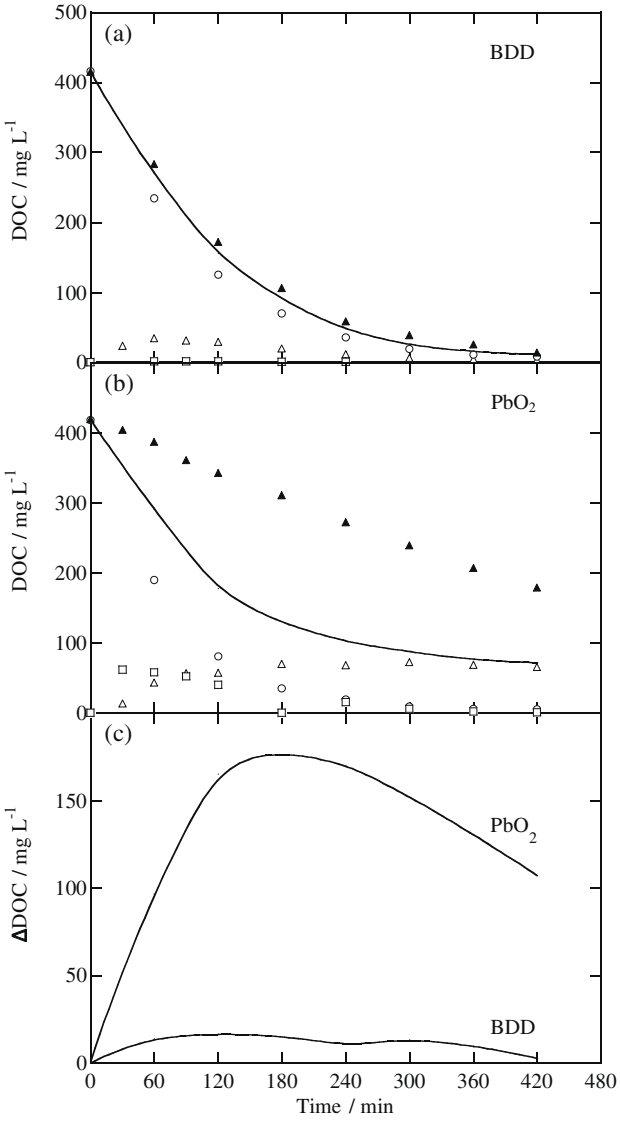

Fig. 5. Evolution of (▲) experimental DOC and calculated values determined for: (○) the remaining initial compound; (□) its aromatic intermediates; and (△) generated carboxylic acids from HPLC analysis during the galvanostatic electrolysis of 1 L of a 534 mg L^{-1} *m*-cresol solution under the conditions given in Fig. 3. The solid line corresponds to the calculated total DOC using a (a) BDD or (b) PbO_2 anode. Plot (c) gives the ΔDOC difference between the measured and calculated DOC for the above trials.

oxidation ability of PbO_2(·OH), which can even evolve to form a precipitate, as detected during this treatment. This behaviour is not strange since oligomers formation from phenol electrooxidation using a PbO_2 anode has been previously reported by us (Belhadj Tahar and Savall, 1998; Belhadj Tahar et al., 2008). Similarly, Panizza et al. (2001) showed that polymeric compounds are produced during the oxidation of 2-naphtol in the potential region of electrolyte stability leading to electrode fouling. However, this process is completely inhibited by electrolyzing with a BDD anode in the potential region of water discharge giving complete incineration of 2-naphtol with electrogenerated BDD(·OH) radicals.

On the basis of the above results, a plausible reaction pathway for *m*-cresol mineralization in acid medium is proposed in Fig. 6. The sequence includes all oxidation by-products identified in the present paper and considers that the main oxidant is the hydroxyl radical generated at each anode. The process starts by direct hydroxylation on the C(4) position of *m*-cresol to yield 2-methylhydroquinone, which is subsequently oxidized to 2-methyl-*p*-benzoquinone. Further degradation of this compounds leads to a mixture of pyruvic, malonic, glycolic, maleic and fumaric acids. The three first by-products are then converted into acetic, tartronic and glyoxylic acids, respectively. Oxidation of these acids, as well as maleic and fumaric, gives oxalic and formic acids, which are finally mineralized to CO_2. Our results make in evidence that ·OH is the oxidant in all reactions using BDD that always lead to mineralization. However, significant differences take place when a PbO_2 anode is used, since a black precipitate is also formed and conversion of acetic into oxalic acid with ·OH at the anode surface becomes very hard (see Fig. 4b). The lower oxidation power of PbO_2 then allows the formation of insoluble polymeric by-products from chemical reaction of several undetected intermediates that are not destroyed with the oxidant.

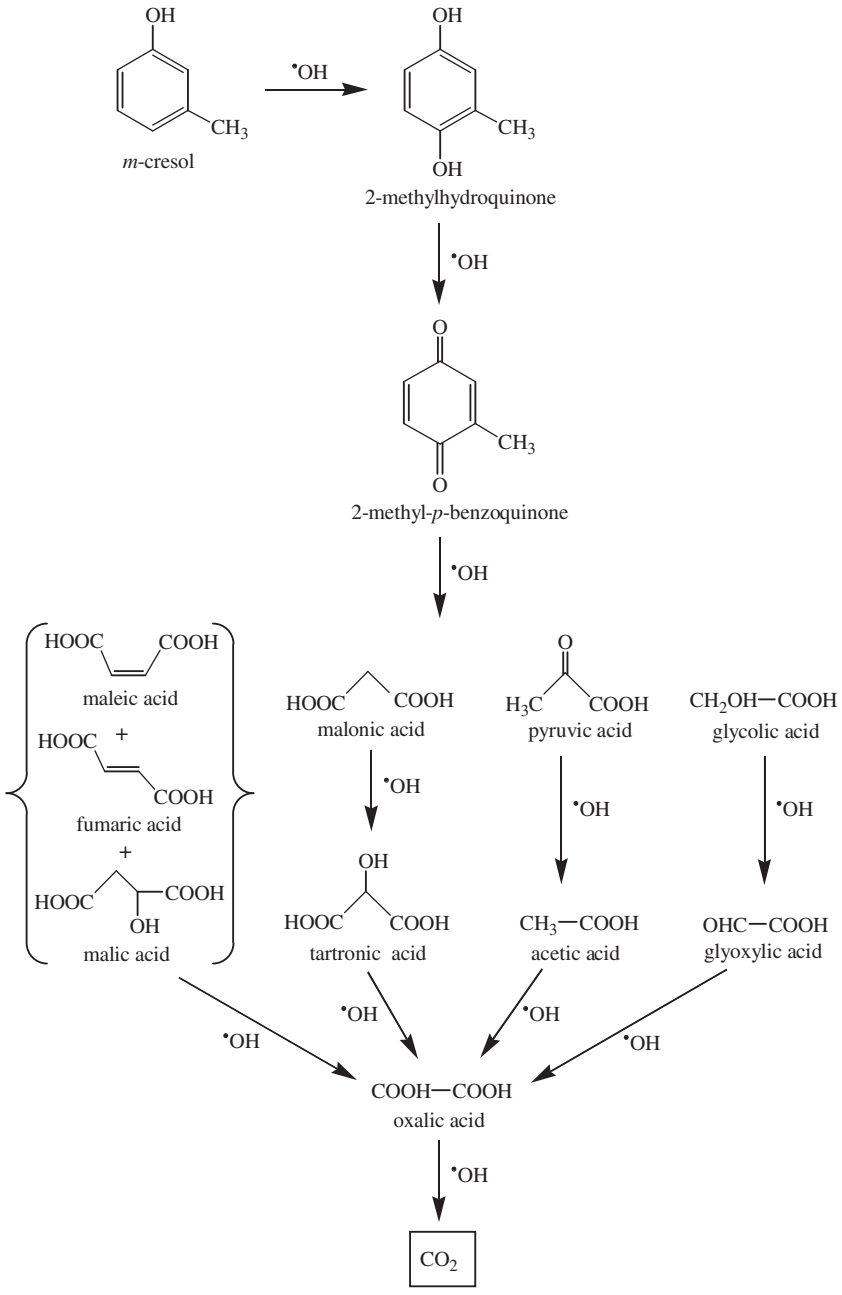

Fig. 6. Proposed reaction pathway for the electrochemical incineration of *m*-cresol in acid medium.

3.4. Energy consumption

The aim of this subsection is to calculate the energy consumption for the electrochemical treatment of the *m*-cresol solutions using the two anodic materials in the present conditions. For an electrochemical reactor operating in galvanostatic conditions at current I (A) during a time t (h), the electrolysis energy E (Wh) is given by the following equation:

$$E = \int_0^t U(t) I \, dt \tag{8}$$

where the cell voltage $U(t)$ (V) can be expressed as the following sum of terms:

$$U(t) = U^0 + \eta_A + \eta_C + \Sigma IR \tag{9}$$

where U^0 is the potential at nil current, η_A and η_C are the corresponding anodic and cathodic overvoltage and (ΣIR) represents the ohmic drop through the solution of resistance R.

The cell voltage was directly measured during the electrolyses of *m*-cresol. A fall of this parameter in the course of the electrochemical process was always observed. However, the decay in $U(t)$ did not exceed 10% in every case, being less important with a BDD electrode. This tendency can be mainly related to the drop of the ohmic drop of the solution, as a consequence of the variation of its composition. At 40 mA cm^{-2}, initial $U(t)$ values of 9.0 and 7.3 V for BDD and PbO_2 anodes, respectively, were determined.

The energy consumption was calculated for the treatment of 1 m^3 of solution considering a plant having the same surface/volume (S/V) ratio for the reactor as that of the laboratory cell (0.0636 cm^{-1}). The electrode surface for such a plant would be 6.36 m^2, obtained, for example, by associating several electrodes in series. While it is currently feasible to dispose PbO_2 electrodes (deposited on titanium) of the order of 1 m^2, the commercially available Si/BDD elements are still much smaller. Keeping the same S/V ratio for the reactor and using the same current density, solution composition and interelectrode gap, the experimentally obtained cell voltage in the laboratory cell can be extrapolated to such upper scale.

The criterion chosen to compare various experiments was based on the toxicity removal. Toxicity is essentially relevant in the presence of aromatic compounds. Indeed, phenol and derivatives are toxic compounds, but quinones stemming from its oxidation are even more (Pulgarin et al., 1994). In our experiments, the solutions were considered as detoxified when the total concentration of aromatics intermediates was less than 1% of the initial *m*-cresol concentration. The removal of aromatics using a BDD anode takes place at the same rate as *m*-cresol disappears. Fig. 2 shows that this situation is reached in about 440 min (corresponding to 18.3 Ah L^{-1}), leading to an energy consumption of 165 kW h m^{-3}. On the other hand, from data of Fig. 3, one can estimate a time of 458 min (corresponding to 19 Ah L^{-1}) as required for 99% aromatic intermediates removal, giving an energy cost of 139 kW h m^{-3} for PbO_2. Although toxicity diminished in the same extent in both cases, it should be noted that DOC removal is much lower using a PbO_2 electrode (190 mg L^{-1} at 19 Ah L^{-1}) compared to a BDD anode (20 mg L^{-1} at 18.3 Ah L^{-1}), where almost complete mineralization is attained. Since similar specific charge is consumed, the greater energy cost using BDD can then be explained by the higher voltage supplied to its electrochemical flow cell.

4. Conclusions

Cresols are degraded at the same rate with a BDD anode whatever the relative position of their $-CH_3$ and –OH groups. Overall electrochemical incineration is attained practically at the same time as the initial pollutant is removed, since BDD(·OH) destroys simultaneously all oxidation by-products formed. The mineralization process of the *m*-cresol effluent on PbO_2 under comparable conditions is much less efficient due to the lower oxidation ability of PbO_2(·OH). Despite this fact, a shorter electrolysis time is needed for the total disappearance of *m*-cresol with PbO_2 than with BDD. The decay kinetics of all cresols on both anodes follows a pseudo-first-order reaction. For *m*-cresol degradation, 2-methylhydroquinone and 2-methyl-*p*-benzoquinone are detected as aromatic intermediates, whereas a mixture of short linear carboxylic acids evolving to oxalic and formic acids as ultimate products are identified and quantified. Acetic acid is very persistent using a BDD anode, but it is largely accumulated with PbO_2, because it cannot be attacked by PbO_2(·OH). Under our experimental conditions, an energy consumption of 165 kW h m^{-3} is needed for achieving the total disappearance of aromatic intermediates, along with almost total mineralization of the *m*-cresol solution, with BDD, which is slightly higher than 139 kW h m^{-3} required for the removal of this pollutant and its aromatic intermediates with PbO_2 giving an effluent with a highly detoxified organic load that may be treated by a post biological treatment.

Acknowledgements

The grant given to C. Flox to do this work and financial support from MEC (Ministerio de Educación y Ciencia, Spain) under project CTQ2007-60708/BQU, co-financed with FEDER funds, are acknowledged.

References

Belhadj Tahar, N., Savall, A., 1998. Mechanistic aspects of phenol electrochemical degradation by oxidation on a Ta/PbO_2 anode. J. Electrochem. Soc. 145, 3427–3434.

Belhadj Tahar, N., Abdelhedi, R., Savall, A., 2008. Study of the electrochemical polymerisation of phenol in aqueous solution on a Ta/PbO_2 anode. J. Appl. Electrochem., in press, doi:10.1007/s10800-008-9760-0.

Boye, B., Dieng, M.M., Brillas, E., 2002. Degradation of herbicide 4-chlorophenoxyacetic acid by advanced electrochemical oxidation methods. Environ. Sci. Technol. 36, 3030–3035.

Brillas, E., Sirés, I., Arias, C., Cabot, P.L., Centellas, F., Rodríguez, R.M., Garrido, J.A., 2005. Mineralization of paracetamol in aqueous medium by anodic oxidation with a boron-doped diamond electrode. Chemosphere 58, 399–406.

Feitelson, J., Hayon, E., 1973. Electron ejection and electron capture by phenolic compounds. J. Phys. Chem. 77, 10–15.

Flezar, B., Plosyznska, J., 1985. An attempt to define benzene and phenol electrochemical oxidation mechanism. Electrochim. Acta 30, 31–42.

Flox, C., Cabot, P.L., Centellas, F., Garrido, J.A., Rodríguez, R.M., Arias, C., Brillas, E., 2006. Electrochemical combustion of herbicide mecoprop in aqueous medium using a flow reactor with a boron-doped diamond anode. Chemosphere 64, 892–902.

Flox, C., Cabot, P.L., Centellas, F., Garrido, J.A., Rodríguez, R.M., Arias, C., Brillas, E., 2007. Solar photoelectro-Fenton degradation of cresols using a flow reactor with a boron-doped diamond anode. Appl. Catal. B: Environ. 75, 17–28.

Flyvbjerg, J., Arvin, E., Jensen, B.K., Olsen, S.K., 1993. Microbial degradation of phenols and aromatic hydrocarbons in creosote-contaminated groundwater under nitrate-reducing conditions. J. Contam. Hydrol. 12, 133–150.

Getoff, N., Schwörer, F., Markovic, V.M., Sehested, K., Nielsen, S.O., 1971. Pulse radiolysis of oxalic and oxalates. J. Phys. Chem. 75, 749–755.

Hatipoğlu, A., San, N., Çinar, Z., 2004. An experimental and theoretical investigation of the photocatalytic degradation of *meta*-cresol in TiO_2 suspensions: a model for the product distribution. J. Photochem. Photobiol. A 165, 119–129.

Kavitha, V., Palanivelu, K., 2005. Destruction of cresols by Fenton oxidation process. Water Res. 39, 3062–3072.

Marselli, B., García-Gómez, J., Michaud, P.A., Rodrigo, M.A., Comninellis, Ch., 2003. Electrogeneration of hydroxyl radicals on boron-doped diamond electrodes. J. Electrochem. Soc. 150, D79–D83.

Martinez-Huitle, C.A., De Battisti, A., Ferro, S., Reyna, S., Cerro-Lopez, M., Quiroz, M.A., 2008. Removal of the pesticide methamidophos from aqueous solutions by electrooxidation using Pb/PbO_2, Ti/SnO_2, and Si/BDD electrodes. Environ. Sci. Technol. 42, 6929–6935.

Martinez-Huitle, C.A., Ferro, S., De Battisti, A., 2004. Electrochemical incineration of oxalic acid. Role of electrode material. Electrochim. Acta 49, 4027–4034.

Nava, J.L., Núñez, F., González, I., 2007. Electrochemical incineration of *p*-cresol and *o*-cresol in the filter-press-type FM01-LC electrochemical cell using BDD electrodes in sulfate media at pH 0. Electrochim. Acta 52, 3229–3235.

Panizza, M., Cerisola, G., 2005. Application of diamond electrodes to electrochemical processes. Electrochim. Acta 51, 191–199.

Panizza, M., Michaud, P.A., Cerisola, G., Comninellis, Ch., 2001. Anodic oxidation of 2-naphtol at boron-doped diamond electrodes. J. Electroanal. Chem. 507, 206–214.
Polcaro, A.M., Mascia, M., Palmas, S., Vacca, A., 2003. Electrochemical oxidation of phenolic and other organic compounds at boron-doped diamond electrodes for wastewater treatment: effect of mass transfer. Ann. Chim. Rome 93, 967–976.
Pulgarin, C., Adler, N., Péringer, P., Comninellis, Ch., 1994. Electrochemical detoxification of a 1,4-benzoquinone solution in wastewater treatment. Water Res. 28, 887–893.
Rajkumar, D., Palanivelu, K., 2003. Electrochemical degradation of cresols for wastewater treatment. Ind. Eng. Chem. Res. 42, 1833–1839.
Rajkumar, D., Palanivelu, K., Balasubramanian, N., 2005. Combined electrochemical degradation and activated carbon adsorption treatments for wastewater containing mixed phenolic compounds. J. Environ. Eng. Sci. 4, 1–9.
Rao, B.H., Asolekar, S.R., 2001. QSAR models to predict effect of ionic strength on sorption of chlorinated benzenes and phenols at sediment-water interface. Water Res. 35, 3391–3401.
Ródenas-Torralva, E., Morales-Rubio, A., de la Guardia, M., 2005. Determination of phenols in waters using micro-pumped multicommutation and spectrophotometric detection: an automated alternative to the standard procedure. Anal. Bioanal. Chem. 383, 138–144.
Savel'eva, O.S., Shevchuk, L.G., Vysotskaya, N.A., 1972. Reactions of substituted phenols with hydroxyl radicals and their dissociated form. O. J. Org. Chem. USSR 8, 283–286.
Serrano, K., Michaud, P.A., Comninellis, Ch., Savall, A., 2002. Electrochemical preparation of peroxodisulfuric acid using boron-doped diamond thin film electrodes. Electrochim. Acta 48, 431–436.
Sirés, I., Brillas, E., Cerisola, G., Panizza, M., 2008. Comparative depollution of mecoprop aqueous solutions by electrochemical incineration using BDD and PbO_2 as high oxidation power anodes. J. Electroanal. Chem. 613, 151–159.
Sivalingam, G., Priya, M.H., Madras, G., 2004. Kinetics of the photodegradation of substituted phenols by solution combustion synthesized TiO_2. Appl. Catal. B: Environ. 51, 67–76.
Wang, K.H., Hsieh, Y.H., Chen, L.J., 1998. The heterogeneous photocatalytic degradation, intermediates and mineralization for the aqueous solution of cresols and nitrophenols. J. Hazard. Mater. 59, 251–260.
Weiss, E., Groenen-Serrano, K., Savall, A., 2008. A comparison of electrochemical degradation of phenol on boron-doped diamond and lead dioxide anodes. J. Appl. Electrochem. 38, 329–337.
Weiss, E., Groenen-Serrano, K., Savall, A., Comninellis, Ch., 2007. A kinetic study of the electrochemical oxidation of maleic acid on boron-doped diamond. J. Appl. Electrochem. 37, 41–47.
Wu, Y., Lerner, D.N., Banwart, S.A., Thornton, S., Pichup, R.W., 2006. Persistence of fermentative process to phenolic toxicity in groundwater. J. Environ. Qual. 35, 2021–2025.
Zhao, G., Shen, S., Li, M., Wu, M., Cao, T., Li, D., in press. The mechanism and kinetics of ultrasound-enhanced electrochemical oxidation of phenol on boron-doped diamond and Pt electrodes. Chemosphere. doi:10.1016/j.chemosphere.2008.08.008.
Zhu, X., Tong, M., Shi, S., Zhao, H., Ni, J., 2008. Essential explanation of the strong mineralization performance of boron-doped diamond electrodes. Environ. Sci. Technol. 42, 4914–4920.